APPLICATION OF THE THREE COMPONENT DECK MODEL TO THE ΛK CHANNEL IN P P REACTION

A.M. ENDLER
M.A. REGO MONTEIRO
A. SANTORO
M. SOUZA

Centro Brasileiro de Pesquisas Físicas - C.B.P.F.
Av. Wenceslau Braz, 71 - 22290 - Rio de Janeiro - R.J. - Brasil

ABSTRACT - We have applied the three-Component-Deck-Model (TCDDM) to the (ΛK) channel in p p reaction. We conclude that our result are very satisfatory and take account the experience. In this paper we take advantage of the fact that spin-structure is the same as (Nπ) channel which has been calculated in previous paper[3].

1. INTRODUCTION

The problem of the diffrative dissociation reactions has been extensively studied lately. The details of the several different approachs can be found in the literature published recently[1].

In spite of the present effort has been oriented to quantum chromodynamics phenomenology we think that this problem, not completely solved, is still very important.

Analysing the recently published data[2] relative to the ΛK channel in p p high energy reaction, we apply the three Component Dual Deck Model (TCDDM)[3] whose results confirm those obtained in other reactions, in particular the slope-mass correlation which is one of the main features of this model. The application to the ΛK channel is straighforward since we have the same spin-parity configuration as in the $N\pi$ channel in p p reaction[3]. We will performe a series of applications which will be a general test to the model to be reported in a forthcoming paper.

Our paper is organized as follows: in part two we describe briefly the (TCDDM). Part three compares the results obtained with the experimental data of reference [2]. Our conclusions and same final remarks follows in part four.

2. THE MODEL - The three component Dual Deck Model (TCDDM)

The authors of the (TCDDM) showed from the analysis of the experimental results [3] (angular correlations , dips on t_2' distributions) that we must consider the three components of a Deck-like model, which correspond to the Born terms of the three possibles exchanges (s,t and u channel) of the subreaction $a + P \to 1 + 2$.

In reference [3] we find a complete and detailed derivation of the model and a comparison with the experimental results on $N\pi$ channel.

We just give a brief description of the (TCDDM) in those aspects relevant to the present paper. The (TCDDM) describes fairly well the experimental results particularly the correlation between M(12) mass versus t_2' (transfer momentum between the target and the final nucleon) and $\cos \Theta^{G.J.}$ (Gottfried-Jackson angle).

Problems which arise from the addition of the three possible exchanges in dual treatment are solved too.

We will apply this model taking in account that to the present reaction

$$p\ p \to \Lambda\ K\ p \qquad (1)$$

the spin-parity configuration is:

$$(1/2)^{+}_{p}\ (1/2)^{+}_{p} \rightarrow (1/2)^{+}_{p}\ (1/2)^{+}_{\Lambda}\ (0^{-})_{K} \qquad (2)$$

The three possibles graphs used to calculate the amplitude are given in figure (1).

We use the general notation $a+b \rightarrow 1+2+3$ where $m_a=m_b=m_3=m$, $m_1=m_\Lambda$ and $m_2=m_K$ are the masses, p_i ($i=a,b,1,2,3$) are the four-momentum which represent each particle.

The squared amplitude to the process (1), calculated under the well known Feynman rules [4],

$$|A|^2 = f_1\,|[ST]|^2 + f_2\,|[SU]|^2 + 2f_3\ \mathrm{Re}\,\{[SU]\,[ST]^*\} \qquad (3)$$

where the [ST] and [SU] terms represent the contributions obtained from the graphs [S], [T] and [U] described above and can be expressed by:

$$[ST] = Z_{st}(s_1-m^2)^{\alpha_K(t_1)-1}\ \Gamma(-\alpha_K(t_1))e^{-i\pi\alpha_K(t_1)} \qquad (4)$$

$$[SU] = Z_{st}(s_1-m^2)^{\alpha_\Lambda(u_1)-1}\ \Gamma(-\alpha_\Lambda(u_1))e^{-i\pi\alpha_\Lambda(u_1)}. \qquad (5)$$

The functions $Z_{st(su)}$ are calculated in reference [3] and they are the "zero" or "dip" equations:

$$Z_{st} = \Sigma_{2b}(s_1-m^2) + \Sigma_{ab}(t_1-m_K^2) \tag{6}$$

$$Z_{su} = \Sigma_{1b}(s_1-m^2) + \Sigma_{ab}(u_1-m_\Lambda^2) \tag{7}$$

where $\Sigma_{ib} = \sigma_{ib}^{\infty} \; e^{B_{ib}\, t_2/2} \qquad i=a,1,2$ (8)

Σ_{ib} represents the Pomeron-exchange parametrization or Pomeron residues in the ib elastic subreactions, where B_{ib} are the slopes and σ_{ib}^{∞} the total asymptotic cross sections.

f_1, f_2 and f_3 are obtained by calculations of the corresponding Feynman graphs for the matrix elements and can be expressed by

$$f_1 = -2t_1 \left[t_2\, m_K^2 + 4(p_b\cdot p_2)\,(p_2\cdot p_3)\right] \tag{9}$$

$$\begin{aligned} f_2 = {} & -2m^2 \left[m_K^2(t_1+t_2) + 4(p_a\cdot p_2)\,(p_1\cdot p_2)\right] - \\ & -4m_K^2 \left[(p_b\cdot p_1)\,(p_a\cdot p_3) + (p_1\cdot p_3)\,(p_a\cdot p_3)\right] + \\ & + 8(p_a\cdot p_2) \left[(p_b\cdot p_1)\,(p_2\cdot p_3) + (p_1\cdot p_3)\,(p_b\cdot p_2)\right] \end{aligned} \tag{10}$$

$$f_3 = t_1 \left[m_K^2 \, t_2 + 4(p_b \cdot p_2)\,(p_2 \cdot p_3) \right] -$$

$$-4(p_a \cdot p_2)\left[(p_a \cdot p_3)(p_b \cdot p_1) + (p_b \cdot p_2)(p_1 \cdot p_3) \right] +$$

$$+ 4(p_1 \cdot p_2) \left[(p_2 \cdot p_3)(p_a \cdot p_b) + (p_b \cdot p_2)(p_a \cdot p_3) \right] \qquad (11)$$

The scalar products in formulas (9), (10) and (11) can be expressed as a function of the invariants:

$$s = (p_a + p_b)^2 \qquad t_{a2} = u_1 = (p_a - p_2)^2$$

$$t_1 = (p_a - p_1)^2 \qquad s_1 = (p_1 + p_2)^2$$

$$t_2 = (p_b - p_3)^2 \qquad s_2 = (p_2 + p_3)^2$$

$$s_3 = (p_1 + p_3)^2$$

We take the Regge trajectories as simple as possible:

$$\alpha_K(t_1) = t_1 - m_K^2 \qquad (12)$$

$$\alpha_\Lambda(u_1) = u_1 - m_\Lambda^2 \qquad (13)$$

with α' fixed to 1 GeV^{-2} .

We can get all distributions from:

$$\sigma = C \int_{\Phi} dt_2 \; ds_1 \; d(\cos\Theta)\, d\phi \; \frac{\lambda^{1/2}(s_1, m_1^2, m_2^2)}{s_1} \; |A|^2 \qquad (14)$$

where A is given by (3) i.e., the amplitude which describes the process, C is a factor which comes from the flux and Jacobian

$$C = 1 \; / \; \left[2^{10} \; \pi^4 \; \lambda\,(s,\, m_a^2,\, m_b^2) \right] \qquad (15)$$

The integration is performed in the physical region Φ . The angles Θ and ϕ are the decay angles of the system (12) in the Gottfried- Jackson or helicity rest frame $\vec{p}_1 + \vec{p}_2 = 0$. The kinematic function λ is done by $\lambda\,(x, y, z) = x^2 + y^2 + z^2 - 2(xy + xz + yz)$.

The present version of (TCDDM) is the so-called Reggeized one in reference [3] . In what follows we will present the results of the model in comparison with the experimental results.

3. COMRARISON WITH THE EXPERIMENTS

We give down a set of figures comparing our theoretical results with the experimental data. Also we present theoretical curves as an exemple of the strong

interferences between the three components in a particular phase space region where the "zeros" are strongest.

We choose conveniently the experimental results from reference [2] which are the most recent to the reaction(1).

Invariant mass M(ΛK) distribution

We have search the best set of parameters to obtain a global comparison with the experimental distributions. As we remarked in reference [3] it is difficult to obtain a good parameter set with the integrated data. We will return to this point in the conclusion.

We take the mass M(ΛK) spectrum to fix the normalization of our distributions (figure (2)). The set of parameters chosen for the off-mass-shell asymptotic total cross section is

$$\sigma_{KN} = 15 \text{ [mb]} \qquad \sigma_{\Lambda N} = 25 \text{ [mb]} \quad \sigma_{NN} = 50 \text{ [mb]}$$

and for the correspondings forward slopes of the elastic subreaction

$$b_{KN} = 4 \text{ [GeV}^{-2}\text{]} \quad b_{\Lambda N} = 7 \text{ [GeV}^{-2}\text{]} \quad b_{NN} = 9 \text{ [GeV}^{-2}\text{]}.$$

Taking in to account the off-mass-shell caracter of each subreaction we think that this values are not incompatible with the experimental values.

Figure [2] shows the results obtained for the (ΛK) mass spectrum using the amplitude calculated by (TCDDM) as described above, where we have taken $P_{lab} = 20$ GeV/c.

$|t_2'|$ distribution $|t_2'| = |t_2 - t_{2\ min}|$

Figure (3) shows the t_2' distributions in each mass interval of the ΛK system. In spite of the experimental errors we think that we reproduce very well both the inflection in the distributions and the global slope-mass correlation.

We remark that the inflections which appears in this $\cos\ \Theta^{G.J.}$ integrated distributions, in t_2', come from the "zero" produced by the three component model.

In order to illustrate the zero which appears in this region we show in figure (3) a theoretical distribution calculated by the (TCDDM) which shows a dear dip to $-0.5 \leq \cos\ \Theta^{G.J.} \leq -0.3$ and two $M(\Lambda K)$ regions $1.61 \leq M \leq 1.7$ and $1.7 \leq M \leq 1.8$.

Figure [4] shows four $\cos\Theta^{G.J.}$ regions for all $M(\Lambda K)$ masses. We note that the region where the "zero" is stronger is for the middle one $|\cos\ \Theta^{G.J.}| \leq 0.5$ and it

is the reflexion of the "zero" showed in figure (5). In the forward region (cos $\Theta^{G.J.} > 0.8$) we see an inflection at $t'_2 \simeq 0$ due to the well known effect of the pseudo - scalar ($p \Lambda K$) vertex which appears in all three components.

We cannot show a complete slope-mass-cos $\Theta^{G.J.}$ correlation as done in reference [3], because there are not experimental curves available.

Angular distributions - **(Θ and ϕ Gottfried-Jackson and helicity frames)**

The distribution presented in figure (6) show a good agreement with the experimental data. There is however a experimental point, at cos $\Theta^{G.J.} \simeq -1$, which we do not understand why in the backward region of a $P \to 12$ we would not see a corresponding baryon exchange peak. This figure (6a) still shows the importance of the baryon exchange for cos $\Theta^{G.J.} \simeq -1$ in our amplitude.

In $\Theta^{G.J.}$ the agreement with the experimental va - lues is very good (fig. 6.b).

We can see also in figure (7) a reasonable agreement with the data. In the region cos $\Theta^{H} \simeq 1$ there is a disagreement with the experimental point which we do not believe it was due to the model. In reference [3] we have discussed this problem which lead us to conclude that our

distribution are correct.

Slope-mass correlation

Figure (8) shows a curve which correspond the slope-mass correlation. In order to obtain this curve we calculate the mean values in intervals for small t_2', which represents the leading slope in the t_2' distributions integrated in all angles.

To compare with the experimental values given in reference [2] we calculated the slope for the same t_2' and M(ΛK) intervals and the results are showed in table I.

4. CONCLUSION

We present a reasonable set of theoretical curves calculated by the(TCDDM)following the formulas described in this paper.

Applying this scheme to the reaction (1) we note that the (TCDDM) describes the main experimental features:

(i) The slope-mass-cos $\Theta^{G.J.}$ correlation to this channel (ΛK).

(ii) Gottfried-Jackson and helicity angular distributions.

(iii) The (ΛK) mass spectrum.

(iv) The t_2' transfer momentum distributions.

There is however a discrepancy showed by the $\cos \Theta^{H}$ distribution for which it is necessary more accurate results in view this disagreement to be the same as the one discussed in reference [3] .

Now we would like to call attention for the choosed set of parameters that we have taken . To understand this problem we make a set of curves in many different regions of $M(\Lambda K)$ and $\cos \Theta^{G.J.}$. In figure (5) we display only the most significant curves regarding this point. We can conclude the following:

(a) The strongest interference appear in the $-0.5 \leq \cos \Theta^{G.J.} \leq -0.3$ region. We still can note that for small $M(\Lambda K)$, near the threshold, the "zero" goes at higher t_2' values when it must be the opposite. Consequently, we can note in figure (8), that the slope-mass correlation is increasing for $1.61 \leq M(\Lambda K) \leq 1.8$ region when it should be decreasing.

(b) The high values obtained for the $\cos \Theta^{G.J.}$ distribution at $\cos \theta^{G.J.} \simeq -1$ (fig.6a) and in $d\sigma/dt_2'$ for $\cos \Theta^{G.J.} \leq -0.5$ at $t_2' \simeq 0$ (fig.4a), are related to the same problem.

(c) It is clear for us that all these problems, mentioned in (a) and (b), come from the choice of the parameters.

We point out once more that the experimentalists who have

at their disposal non integrated data should be able to performe an optimization in order to find the best set of parameters to our amplitude. For the theoreticians it is very difficult to obtain a good set of parameters that take into account all distributions with the integrated data due to computational reasons.

We intend to apply this model in the $(\Delta^{++}\ \pi^{-})$ channel for the same initial reaction and afterwards to make a systematic and complete study of the slope-mass - $\cos\ \Theta^{G.J.}$ correlation for all diffractive dissociation reactions. We acknowledge Dr. A. Olinto for the carefull reading of the manuscript.

REFERENCES

[1] A.B. Kaidalov - Physics Reports, 50, 157, (1979)
L.A. Ponomarev, I.T.E.P., 18, (1977)

[2] Bonn-Hamburg- München - (MPI) - Collaboration, N.P. 125B, 423, (1977)

[3] (a) G. Cohen-Tamoudgi, A. Santoro and M. Souza, N.P. 125B, 445, (1977)
(b) F.Hayot, A. Morel, A. Santoro and M. Souza, N.C. Letters, 18, 185, (1977)

[4] J.D. Bjorken and S.D. Drell - Relativistic Quantum mechanics - Mc Graw-Hill Book Company N.Y. - U.S.A.

FIGURE CAPTIONS

TABLE I: Comparison of the theoretical and experimental values obtained for the slope B (GeV^{-2}) is some $M(\Lambda K^+)$ range. The experimental values in this table were taken from reference [2] and the theoretical values B (GeV^{-2}) are the results obtained by the model. Note that the used t_2' intervals to calculated the slopes B are too large.

FIGURE 1: The (TCDDM) graphs for reaction (1)

(a): K exchange

(b): Λ exchange

(c): direct graph

FIGURE 2: The mass distribution of the (ΛK^+) system. The full line shows the result of the (TCDDM).

FIGURE 3: $\frac{d\sigma}{dt_2'}$ distribution for various $M(\Lambda K^+)$ intervals, integrated over all $\cos\Theta^{G.J.}$ and $\phi^{G.J.}$

(a): for all $M(\Lambda K)$ masses

(b): for $1.61 \leq M(\Lambda K) \leq 1.8$ GeV

(c): for $1.8 \leq M(\Lambda K) \leq 2.0$ GeV

(d): for $2.0 \leq M(\Lambda K) \leq 2.5$ GeV

FIGURE 4: $\frac{d\sigma}{dt_2'}$ distribution for some $\cos\Theta^{G.J.}$ regions for all masses of ΛK^+ system and integrated over all $\phi^{G.J.}$

(a): In the interval $\cos\Theta^{G.J.} < -0.5$

(b): for $|\cos\Theta^{G.J.}| \leq 0.5$

(c): $\cos\Theta^{G.J.} \geq 0.8$ (full line)

$\cos\Theta^{G.J.} \geq 0.5$ (doted line)

FIGURE 5: Theoretical $d\sigma/dt_2'$ distribution calculated by (TCDDM).

(a): In the interval $1.61 \leq M(\Lambda K) \leq 1.7$ [GeV] and $-0.5 \leq \cos\Theta^{G.J.} \leq -0.3$

(b): In the interval $1.7 \leq M(\Lambda K) \leq 1.8$ [GeV] and $-0.5 \leq \cos\Theta^{G.J.} \leq -0.3$

FIGURE 6: Gottfried-Jackson angles distributions for all masses and for $0 \leq |t_2'| \leq 1$

(a): $\cos\Theta^{G.J.}$ distribution integrated in all $\phi^{G.J.}$

(b): $\phi^{G.J.}$ distribution integrated in all $\cos\Theta^{G.J.}$

FIGURE 7: Helicity angles distributions for all masses and for $0 \leq |t_2'| \leq 1$.

(a): $\cos\Theta^{H}$ distribution integrated over all ϕ^{H}.

(b): ϕ^{H} distribution integrated over all $\cos\Theta^{H}$.

FIGURE 8: The theoretical slope-mass correlation.

TABLE I

$M(\Lambda K^+)$ RANGE (GeV)	t_2' RANGE (GeV^2)	B exp. (GeV^{-2})	B theo. (GeV^{-2})
ALL $M(\Lambda K^+)$	$0. \leq t_2' \leq 0.40$	6.2 ± 1.5	7.06
$M(\Lambda K^+) \leq 1.8$	$0. \leq t_2' \leq 0.32$	11.2 ± 3.4	9.05
$1.8 \leq M(\Lambda K) \leq 2.0$	$0. \leq t_2' \leq 0.40$	6.1 ± 2.4	7.43
$M(\Lambda K) \geq 2.0$	$0. \leq t_2' \leq 0.40$	4.8 ± 2.9	5.32
$M(\Lambda K) < 2.0$ $\cos \Theta^{G.J.} < 0$	$0. \leq t_2' \leq 0.32$	10.4 ± 2.9	14.56
$M(\Lambda K) < 2.0$ $\cos \Theta^{G.J.} > 0$	$0. \leq t_2' \leq 0.32$	6.5 ± 1.9	4.83

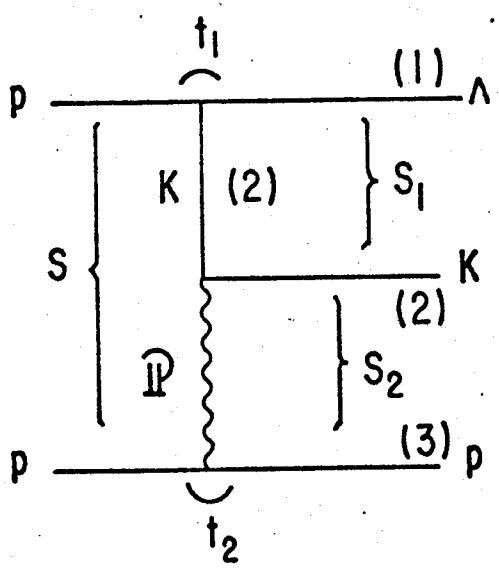

(a)

[T]

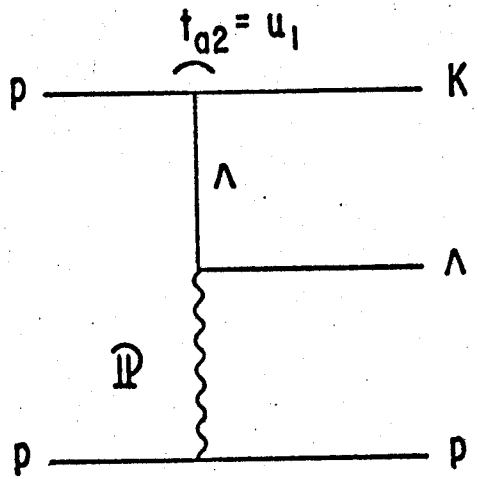

(b)

[U]

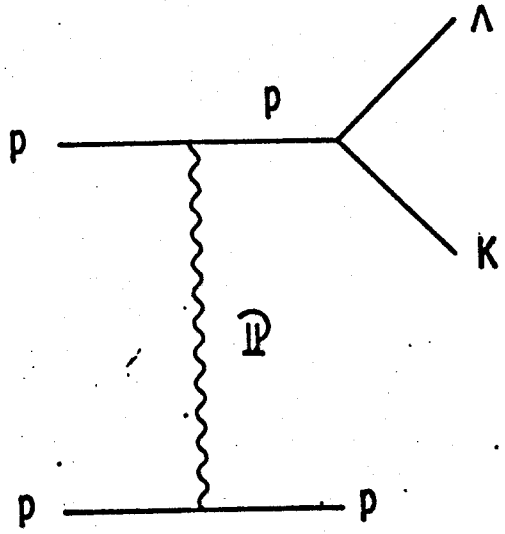

(c)

[S]

(Fig. 1)

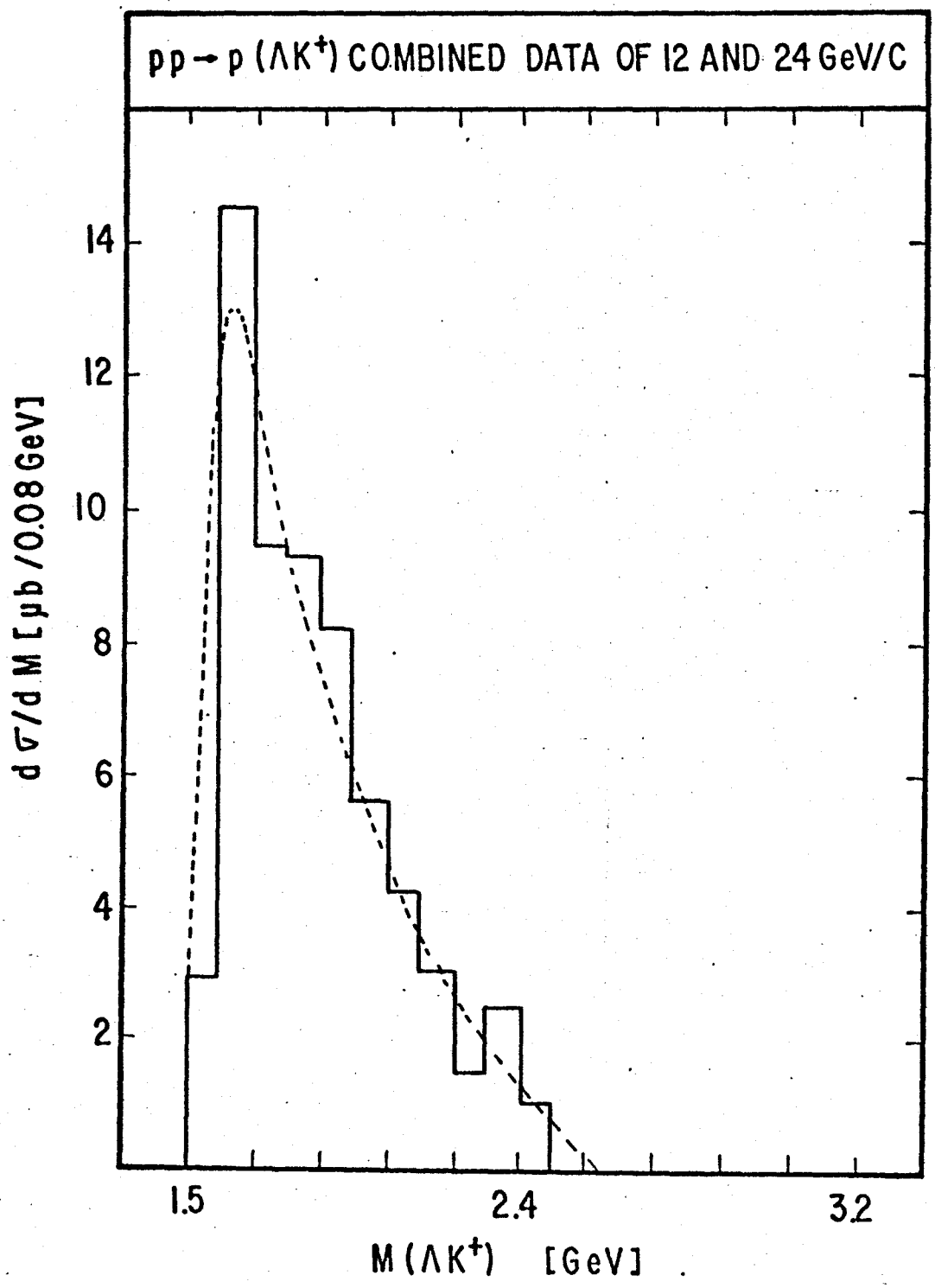
pp → p (ΛK+) COMBINED DATA OF 12 AND 24 GeV/C
dσ/dM [μb/0.08 GeV]
14
12
10
8
6
4
2
1.5
2.4
3.2
M(ΛK+) [GeV]

(Fig. 2)

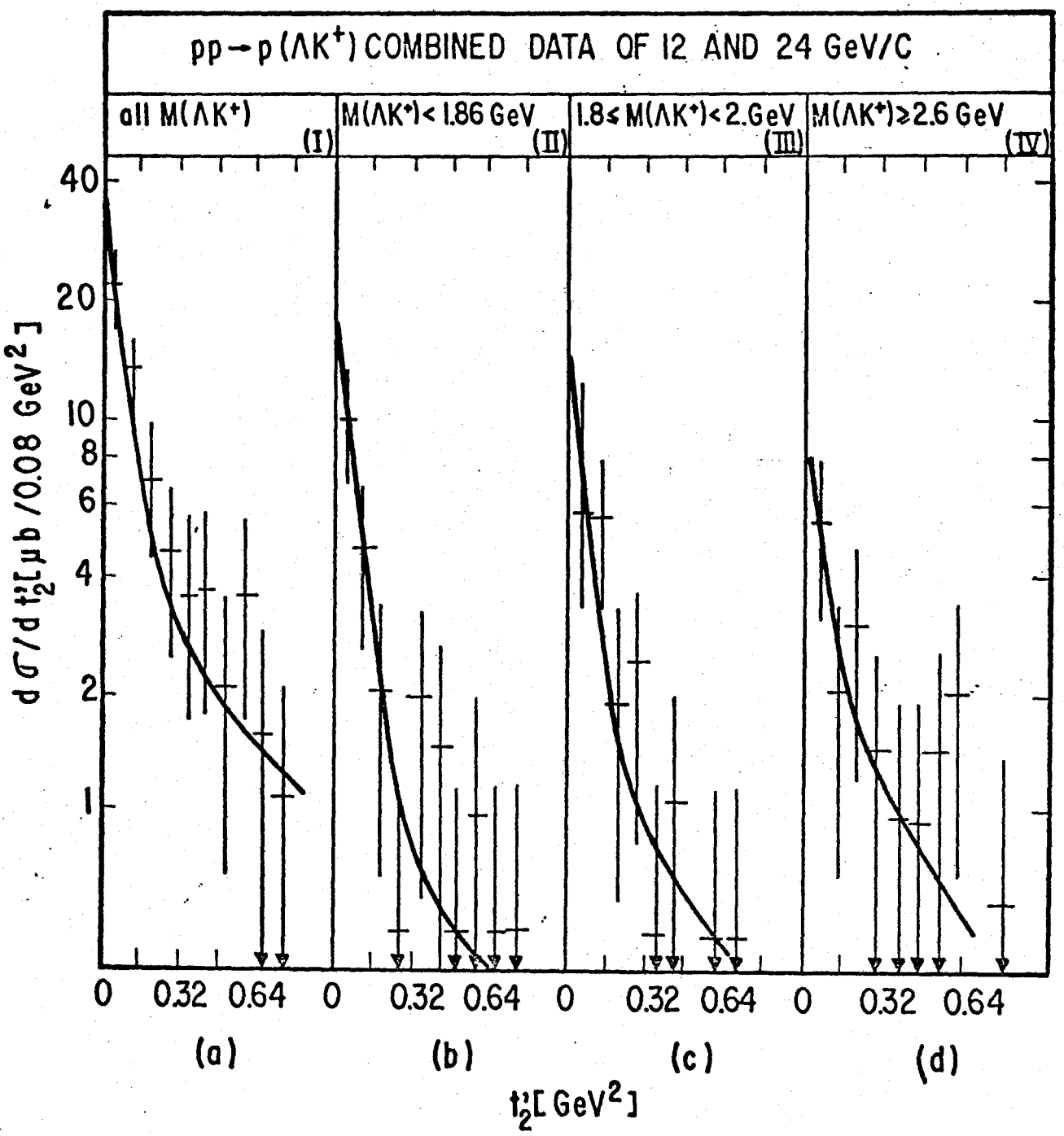
pp → p(ΛK+) COMBINED DATA OF 12 AND 24 GeV/C
all M(ΛK+) (I)
M(ΛK+)< 1.86 GeV (II)
1.8≤ M(ΛK+)< 2.GeV (III)
M(ΛK+)≥2.6 GeV (IV)
dσ/dt'2[μb/0.08 GeV2]
40
20
10
8
6
4
2
1
0
0.32
0.64
(a)
(b)
(c)
(d)
t'2[GeV2]

(Fig. 3)

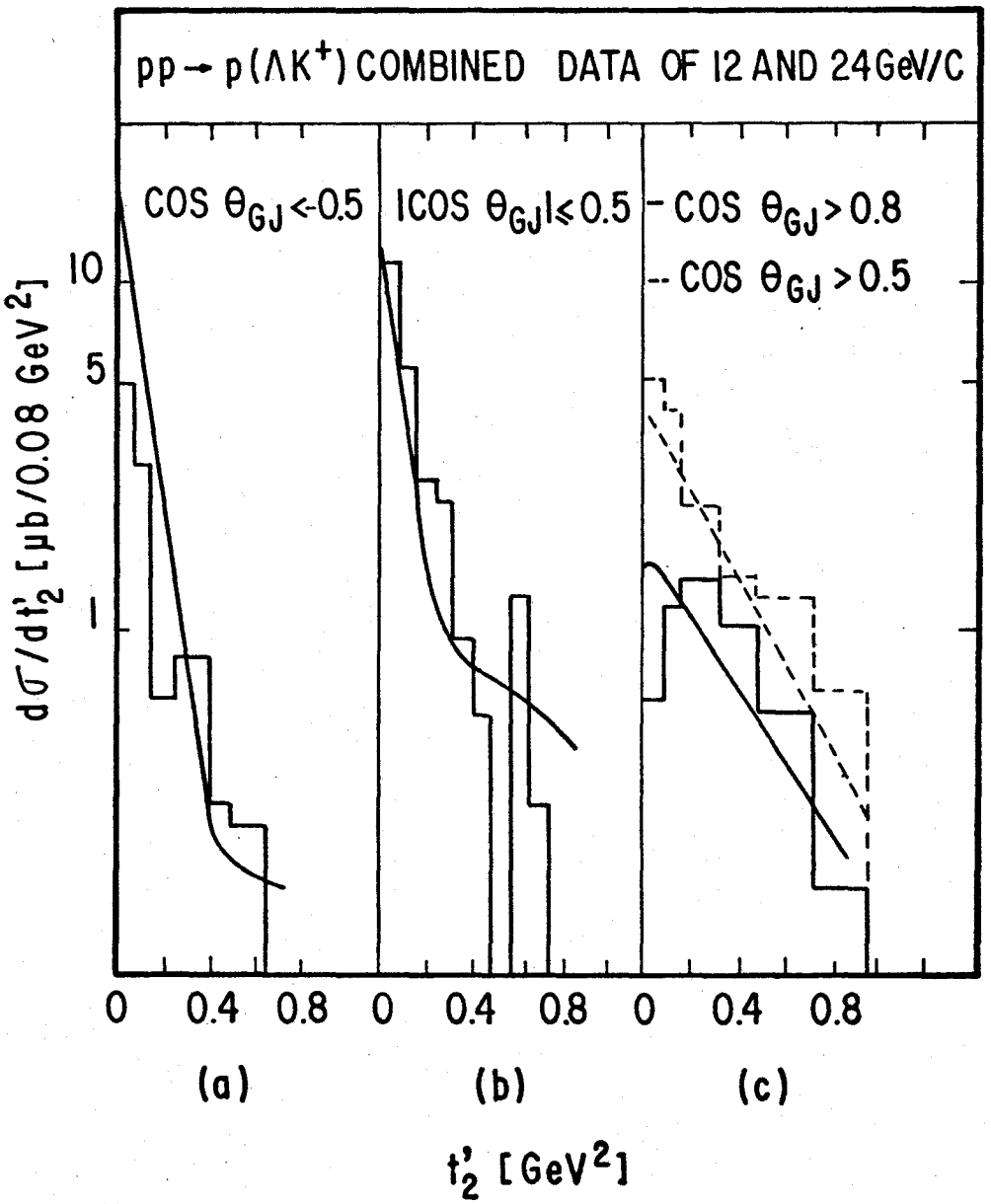
pp → p(ΛK+) COMBINED DATA OF 12 AND 24GeV/C
COS θGJ<-0.5
ICOS θGJI≤0.5
- COS θGJ>0.8
-- COS θGJ>0.5
dσ/dt'2 [μb/0.08 GeV2]
10
5
1
0
0.4
0.8
(a)
(b)
(c)
t'2 [GeV2]

(Fig. 4)

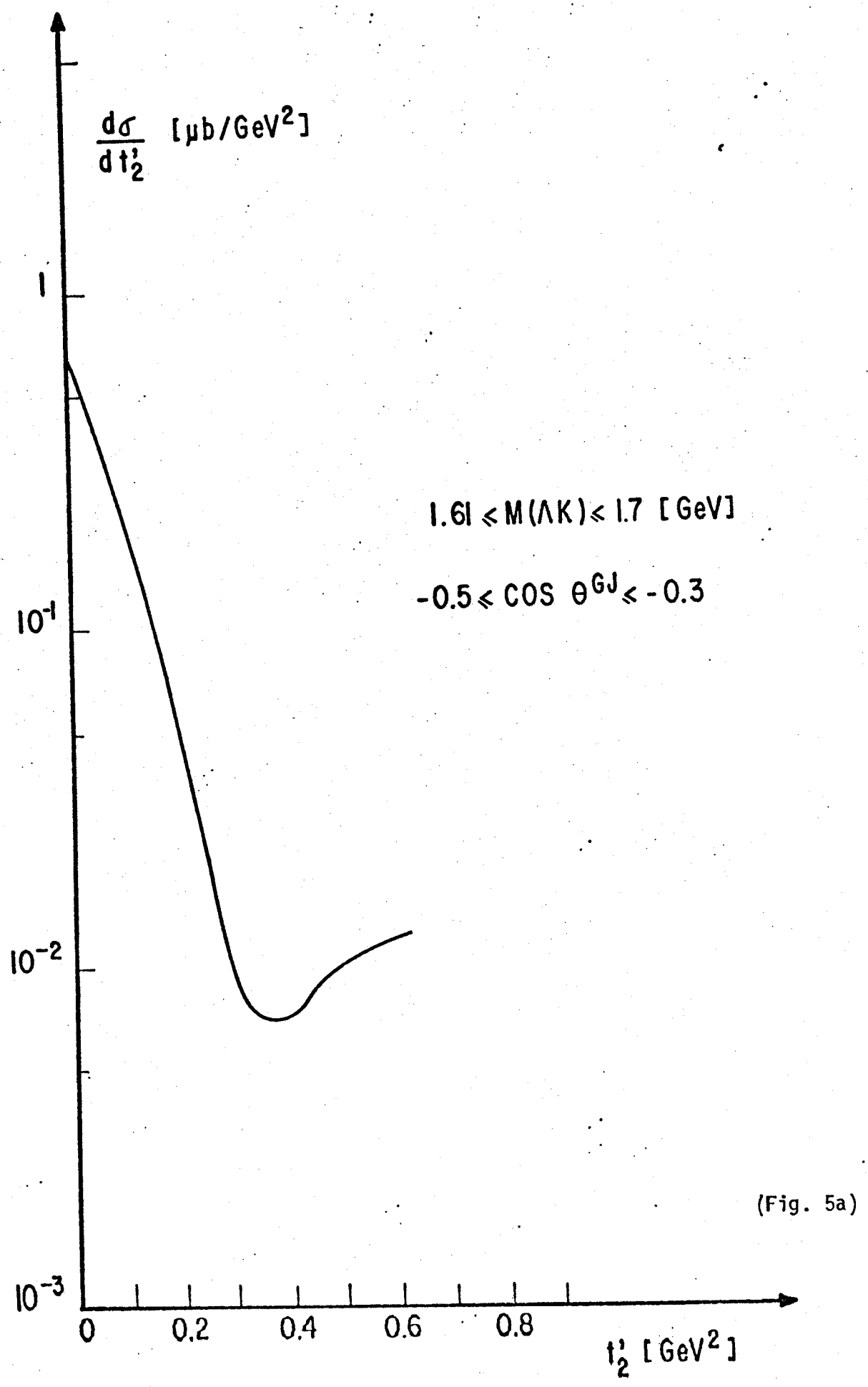
$\frac{d\sigma}{dt_2'}$ [μb/GeV²]
1
10^{-1}
10^{-2}
10^{-3}
0
0.2
0.4
0.6
0.8
t_2' [GeV²]
1.61 ≤ M(ΛK) ≤ 1.7 [GeV]
-0.5 ≤ COS θ^{GJ} ≤ -0.3

(Fig. 5a)

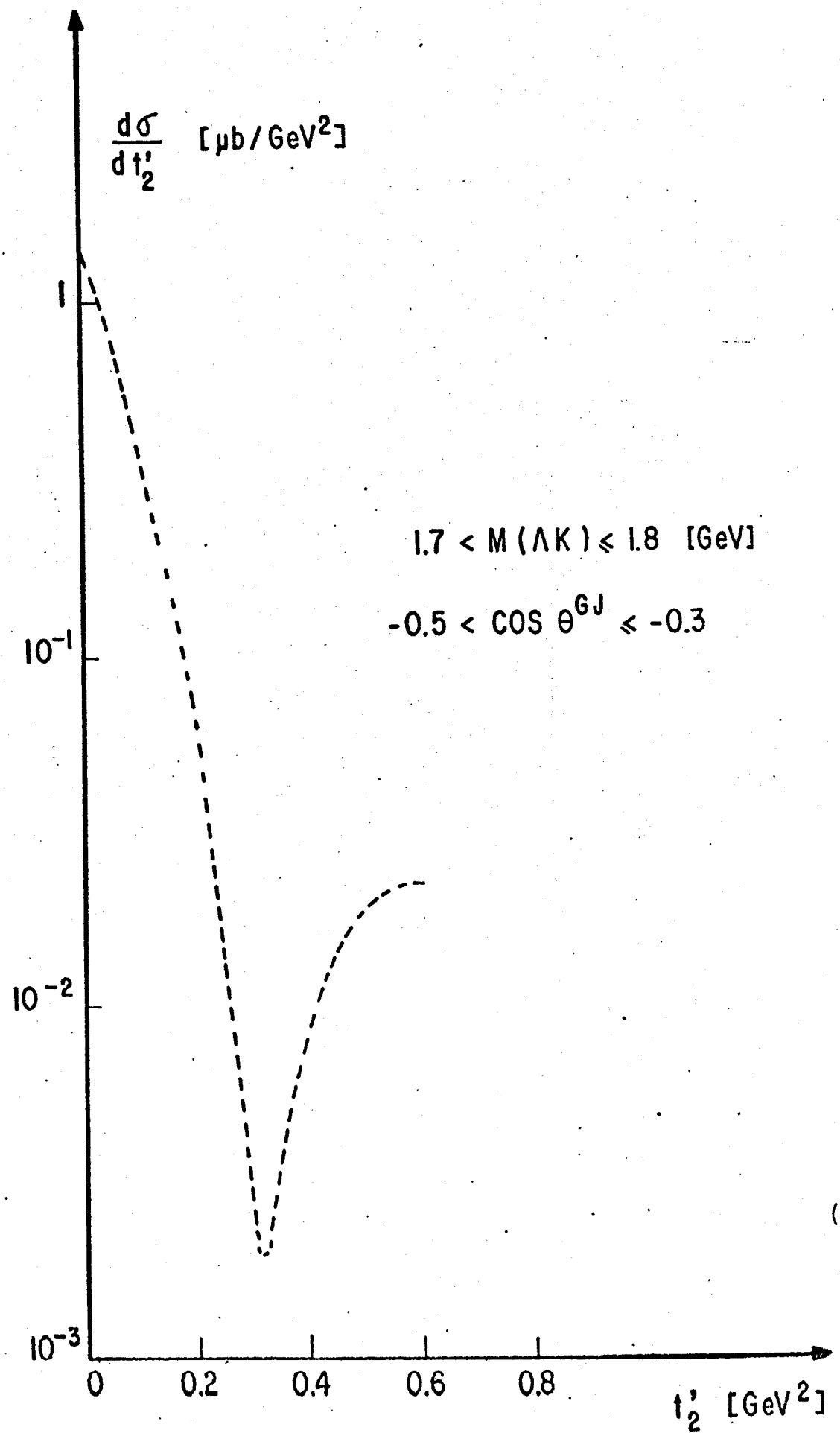
$\frac{d\sigma}{dt_2'}$ [μb/GeV²]
1
10^{-1}
10^{-2}
10^{-3}
0
0.2
0.4
0.6
0.8
t_2' [GeV²]
1.7 < M(ΛK) ≤ 1.8 [GeV]
-0.5 < COS θ^{GJ} ≤ -0.3

(Fig. 5b)

$pp \rightarrow p(\Lambda K^+)$ COMBINED DATA OF 12 AND 24 GeV/C

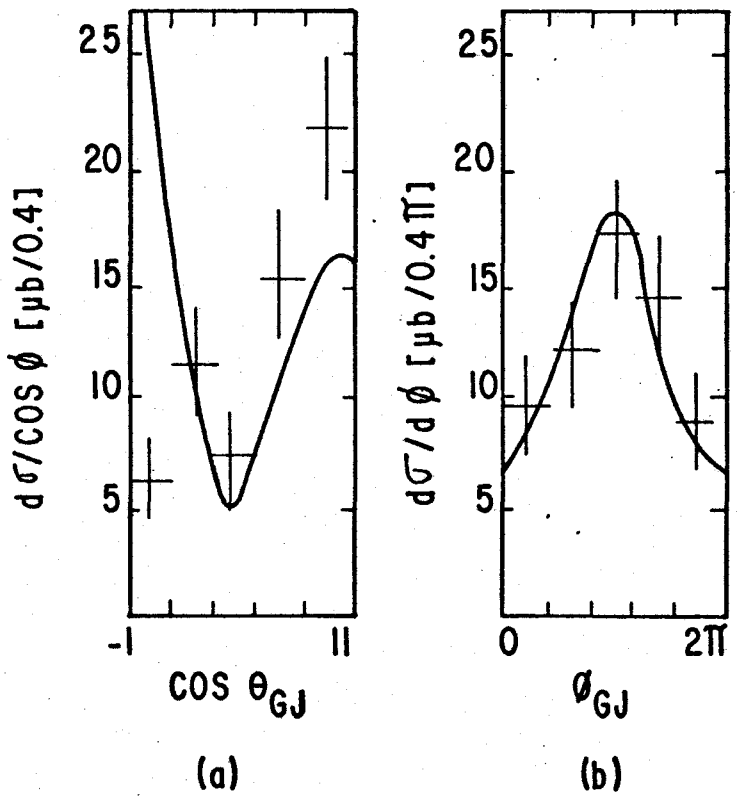

(Fig. 6)

$p\,p \rightarrow p\,(\Lambda K^{+})$ COMBINED DATA OF 12 AND 24 GeV/C

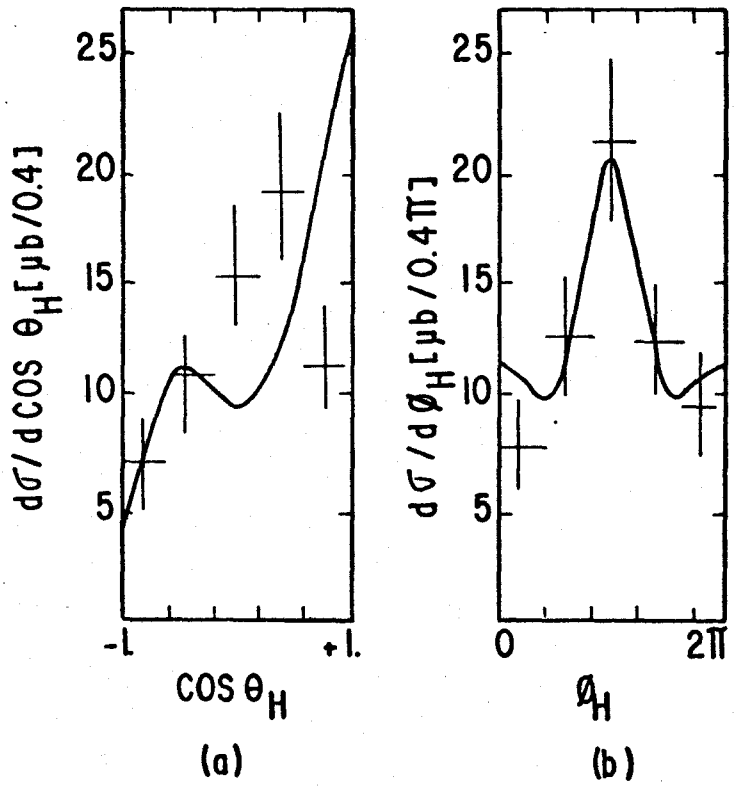

(Fig. 7)

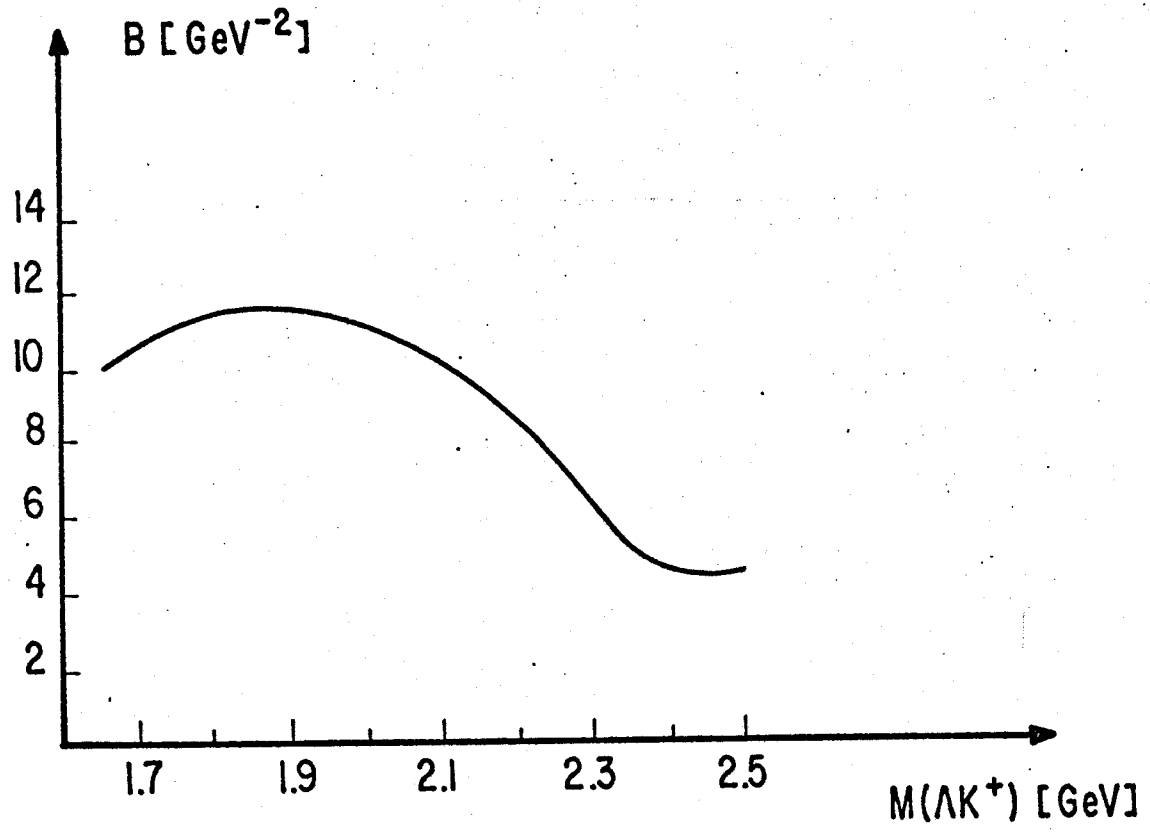

(Fig. 8)